Magnetic Resonance Imaging 56 (2019) 144–150

Contents lists available at ScienceDirect

Magnetic Resonance Imaging

journal homepage: www.elsevier.com/locate/mri

Original contribution

Two-dimensional nuclear magnetic resonance method for wettability determination of tight sand

Can Liang[a], Lizhi Xiao[a,b,*], Cancan Zhou[c], Yan Zhang[a], Guangzhi Liao[a], Zijian Jia[a]

[a] State Key Laboratory of Petroleum Resources and Prospecting, China University of Petroleum, Beijing 102249, China
[b] Harvard SEAS-CUPB Joint Laboratory on Petroleum Science, 29 Oxford Street, Cambridge, MA 02138, USA
[c] Research Institute of Petroleum Exploration and Development, Beijing 100083, China

ARTICLE INFO

Keywords:
Nuclear magnetic resonance (NMR)
Diffusion-transverse relaxation time (D-T_2) maps
Internal gradients
Wettability characterization
Tight sand

ABSTRACT

The wettability of reservoir rocks is important for oil recovery and reserve calculations. However, current methods for evaluating the wettability of rocks are time-consuming and expensive. Previous work has shown that low-field nuclear magnetic resonance (NMR) is a potentially useful and non-invasive technique for rock wettability determination. However, for rocks with strong internal magnetic field gradients, the current method is less efficient. In this study, the bipolar pulsed field gradient (PFG)-Carr-Purcell-Meiboom-Gill (CPMG) pulse sequence was applied to the study of rock wettability. This method can suppress the effect of the internal magnetic field gradient in rocks and accurately extract wettability information. The diffusion-transverse relaxation time (D-T_2) method was employed to quantitatively estimate the wettability of rocks. Results of Amott wettability tests and NMR T_1-T_2 maps were combined to provide a more complete wettability characterization of tight sand. The results demonstrate the feasibility of the new method for characterizing wettability. The proposed method and workflow is of significance to the development of oil fields.

1. Introduction

Wettability is one of a few critical petrophysical properties, which is fundamental to reservoir description and engineering. Its inaccuracies can lead to errors in logging-based fluid saturation analyses and even incorrect assessments of petroleum reserves. The present industrial methods, namely, Amott or U.S. Bureau of Mines (USBM) tests, are time-consuming and limited to laboratory use. Thus, the measurement of rock wettability remains challenging.

Nuclear magnetic resonance (NMR) is widely used in the petroleum industry for rock analysis. In 1992, the fundamental connection between wettability and NMR spin relaxation was introduced in detail by Hsu et al. [1,2]. This formed the basis for NMR wettability research [3]. Subsequently, many studies have been performed on porous media or rock samples using NMR techniques, and these studies have shown that relaxometry and diffusion offer potential methods for analyzing fluid distributions and wettability [4–6]. However, reservoir rocks are very complicated, especially in tight formations. The various minerals, complex pore structures, and heterogeneous wettability may cause heterogeneity in magnetic susceptibility, which induces strong internal magnetic field gradients [7]. The internal gradients intensities are roughly inversely proportional to the pore size and scale linearly with the applied field strength expressed as $\Delta\chi B_0$, where $\Delta\chi$ is the magnetic susceptibility difference between the fluid and pore surface, and B_0 is the applied magnetic field [8]. Such internal gradients can introduce bias in transverse relaxation and diffusion measurements as a result of the extra dephasing of the signal. For example, decreases in transverse relaxation time (T_2) arise from translational diffusion through the internal gradients as described in Eq. (1).

Conventional diffusion and relaxation (D-T_2) measurements using the pulsed field gradient (PFG) - Carr-Purcell-Meiboom-Gill(CPMG) pulse sequence with unipolar gradients were influenced by internal gradients [9]. Chen et al. [10] and Minh et al. [11] mentioned that D-T_2 maps obtained from this method added uncertainty to the established wettability values. In our previous work, we used spin echo (SE) and CPMG for D-T_2 correlation data to establish NMR wettability indices [12]. However, it was found the results of rocks with strong internal gradients cannot correlate well with the Amott tests, which indicates that a further study is required.

It is necessary that the effects of internal gradients are taken into consideration for rock wettability evaluation. Especially for reservoir rocks characterized with chlorite films or iron minerals, diffusion measurements are complicated, and potentially inaccurate data can be obtained using conventional NMR methods due to the background

* Corresponding author at: State Key Laboratory of Petroleum Resources and Prospecting, China University of Petroleum, Beijing 102249, China.
E-mail address: xiaolizhi@cup.edu.cn (L. Xiao).

https://doi.org/10.1016/j.mri.2018.09.020
Received 30 July 2018; Received in revised form 17 September 2018; Accepted 18 September 2018

gradients in these materials. Cotts et al. [13] developed the modified PFG-stimulated echo (STE) sequence with pairs of bipolar gradients to vanish the cross term between the background gradient and applied gradients. This PFG-STE-Bipolar-CPMG pulse sequence can suppress the effect of the internal magnetic field gradient in rocks and isolate the influence of wettability alone. In this work, this sequence was applied to investigate rock wettability.

The aim of this study is to obtain more accurate wettability information for tight sands by using low-field NMR. We took advantage of CPMG and bipolar PFG-STE methods to obtain D-T_2 correlation data on samples. The industrial tests and NMR-based wettability results agreed well. In addition, T_1-T_2 relaxation correlation data were analyzed to complement qualitative wettability interpretations. The workflow presented revealed that rock wettability can be evaluated with low-field NMR.

2. Theory

2.1. Methodology

The NMR technique has been extensively applied to the characterization of porous media. In the petroleum industry, the CPMG transverse relaxation measurement as a standard NMR method is used to assess porosity and pore size distribution of rocks. It has been adopted as a rapid and robust approach that can be performed in the borehole. The T_2 relaxation of porous media saturated with low-viscosity fluid is described by the following equation:

$$\frac{1}{T_2} = \frac{1}{T_{2Bulk}} + \rho_2\frac{S}{V} + \frac{D\gamma^2G^2T_E^2}{12}, \tag{1}$$

where S is the pore surface area, V is the volume of the pores, ρ_2 is the surface relaxivity for T_2, γ is the gyromagnetic ratio, D is the diffusion coefficient of the fluid, T_E is the echo spacing and G is the magnetic field gradient. Because of the presence of internal gradients, a small T_E is applied. In conventional rock systems, the relaxation time distribution is determined by the surface-to-volume ratio and surface area material in the presence of saturating wetting fluid. The relaxation interpretation is complicated because of the presence of multiphase fluids. Thus, the diffusivity of various liquids is simultaneously decoded via NMR techniques for fluid separation. In typical diffusion experiments with SE or STE sequences, the systematic error caused by the presence of a cross term between the background gradient, g_{int}, and the applied gradient, g_a, can produce inaccurate diffusion measurements [13,14].

For clastics (sandstones), especially tight sand, it has been found that rock matrix minerals, quartz, and feldspar are coated by a chlorite film, even pore-lining chlorite as shown in Fig. 2. The internal gradients in these rocks are large. Leu et al. [9] compared rock results of strong g_{int} and negligible g_{int} with the fixed and pulsed gradient diffusion methods in low-field NMR. It was suggested that there was a need to cancel the effects of the internal gradients of the inhomogeneous porous media. Therefore, a modified STE with bipolar gradient pairs (Fig. 1) was applied to acquire accurate diffusion and relaxation information. This provides a better signal-to-noise ratio (SNR) due to the absence of internal gradients. However, this signal gain may be counteracted by a more rapid signal decay of a lower T_2 less than 1 ms in our experimental setup. This method can be used for constructing D-T_2 correlation maps and $f(D, 1/T_2)$ using Eq. (2), where $\triangle$ is the diffusion time and the spin storage time; δ is the duration of an applied gradient pulse appearing between two radiofrequency (RF) pulses. Usually, $\triangle \gg \delta$. During the CPMG period, T_2 encoding is performed at short echo time τ_2 so that signal attenuation by diffusion can be neglected. The kernel for this sequence is described as below:

$$K_1(D,\delta)\cdot K_2(T_2, nT_E) = \exp\left(-\gamma^2 g_a^2(2\delta)^2 D\left(\Delta - \frac{\tau_1}{2} - \frac{\delta}{6}\right)\right) \times \exp\left(-\frac{t}{T_2}\right) \tag{2}$$

The T_1-T_2 correlation is measured by using the inversion recovery CPMG pulse sequence for the local wettability analysis based on the relaxation theory from Korb et al. [15,16]. It bridges the adsorption ability and T_1/T_2 ratio even in low-field NMR. Valori et al. [17] concluded that the T_1/T_2 ratio of the wetting phase increased relative to the bulk value. An excellent correlation between the T_1/T_2 of the oil signal and wettability index was demonstrated in carbonate rock core plugs with refined oil and doped water. This technique was then applied to tight sand. It was found that the T_1/T_2 ratio of the wetting fluid was greater than that of the non-wetting phase, which was rarely $T_1/T_2 = 1$ in tight rocks. Therefore, use of this method as a complement provides additional qualitative wettability information that can be useful for interpretations.

2.2. Predicting wettability

The wetting feature determines the relaxation behavior of fluids in a porous material. Theoretically, the wetting fluid influences the surface relaxation behavior since it is in contact with the pore walls. The non-wetting fluid has a relaxation rate similar to that of the bulk fluid. Thus, the T_2 distribution in an oil-water system with a uniform water-wet state will contain bulk and surface relaxation characteristics of water and oil, respectively. The relative surface area of pore-filling water contact defines the NMR wettability index as described by Fleury and Deflandre [18],

$$I_{NMR} = \frac{\left(\frac{1}{T_{2,w}} - \frac{1}{T_{2,bw}}\right)\cdot S_w - \left(\frac{1}{T_{2,o}} - \frac{1}{T_{2,bo}}\right)\cdot S_o\cdot\left(\frac{\rho_{2,w}}{\rho_{2,o}}\right)}{\left(\frac{1}{T_{2,w}} - \frac{1}{T_{2,bw}}\right)\cdot S_w + \left(\frac{1}{T_{2,o}} - \frac{1}{T_{2,bo}}\right)\cdot S_o\cdot\left(\frac{\rho_{2,w}}{\rho_{2,o}}\right)}, \tag{3}$$

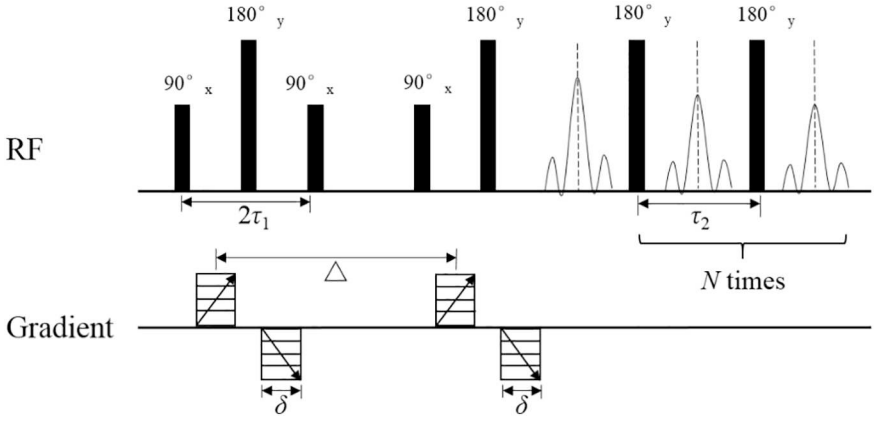

Fig. 1. PFG-STE-Bipolar-CPMG pulse sequence.

where I_{NMR} is scaled from −1 for an oil-wet condition, to +1 for a fully water-wet condition, $T_{2,w}$ and $T_{2,o}$ are the observed relaxation time of water and oil, respectively, $T_{2,bw}$ and $T_{2,bo}$ are the known fluid bulk relaxations, and S_w and S_o represent water and oil saturation, which are acquired by weighing or measuring the displaced fluid volume in laboratory experiments. The surface relaxivity of the saturating water and oil is denoted as ρ_w and ρ_o, which are satisfied with the diffusion equation using the Padé approximant extrapolation, which is written as follows [19]:

$$D(T_2) = D_0\left(1 - \gamma\frac{\alpha L_D + \left(\frac{L_D}{L_M}\right)^2}{\alpha L_D + \left(\frac{L_D}{L_M}\right)^2 + \gamma}\right), \quad (4)$$

where $\alpha = \frac{4}{9\sqrt{\pi}}\cdot\frac{1}{T_2}\cdot\frac{1}{\rho_{eff}}$, $\gamma = 1 - \phi^{m-1}$, and $L_D = \sqrt{D_0 T_D}$; φ is the porosity, m is the Archie cementation exponent, and L_M is the heterogeneity length scale of the medium, usually $L_M \gg L_D$. The diffusion encoding time is T_D. The surface relaxivities are obtained as fitting parameters from Eq. (4). Mathematically, when the difference between the generalized diffusion function $D(T_2, \rho)$ and the diffusion coefficient log mean (DCLM) of the D-T_2 map reaches a minimum value, the optimum solution is an appropriate effective surface relaxivity ρ_{effw} or ρ_{effo}. Finally, the NMR wettability index I_{NMR} can be determined by combing other relaxation parameters in Eq. (3).

3. Experimental section

3.1. Samples

The samples used in this study were tight oil sands. These samples were collected from drill core taken in western China. The samples had a small porosity range from 8 to 15 pu, and permeability was less than 10 mD.

The NMR measurements of the samples were performed on a 2 MHz Rock Core Analyzer (Magritek, New Zealand). Tight sand samples were cut in 1 in. diameter and less than 2 in. height. The susceptibility contrasts $\Delta\chi$ of the samples are reflected in the mono-exponential fit of free induction decay (FID), of which the magnitude decay rate $1/T_2^*$ satisfies the product of the susceptibility contrast and field strength as $1/T_2^* \approx \gamma\Delta\chi B_0$ [20]. Results for the two samples discussed below were 41.31×10^{-6} SI and 69.16×10^{-6} SI. The internal gradient distributions, measured by the CPMG sequence that capitalizes upon the decreasing echo amplitude as a function of increasing echo spacing T_E in a constant relaxation time nT_E [21], are presented in Fig. 2. Sample B exhibited a right shift toward a higher internal field gradient compared to sample A. This finding conforms to susceptibility contrasts results and the scanning electron microscopy (SEM) results whereby the majority of pore spaces contained clay minerals in sample B. The flake clay minerals and iron-bearing material contributed to the heterogeneous solid compositions of the tight sand.

3.2. Experimental protocol

The experimental process was designed as shown in Fig. 3. After ageing the cores via oil-displacement, an Amott test was performed. The NMR relaxation and diffusion were measured at different saturation states of the samples. For both D-T_2 and T_1-T_2 measurements of the samples, the echo spacing was 200 μs. For the diffusion experiments, when the samples were saturated with water, the pulsed field gradients strength g_a varied from 0 to 0.5 T/m linearly, and a stimulated echo with a gradient pulse duration $\delta = 1.5$ ms and a diffusion time $\triangle = 20$ ms was applied. Meanwhile $\delta = 3$ ms and $\triangle = 30$ ms were employed to measure the low diffusion coefficient for oil in samples filled with oil and water. The scanning number was set as 256 to improve the SNR to ~16. For the T_1-T_2 experiments, the T_1 encoding time was logarithmically varied from 0.5 to 3000 ms in 20 steps.

4. Results and discussion

4.1. Two-dimensional measurements

As shown in Figs. 4 and 5, the D-T_2 and T_1-T_2 maps at different saturation states for the two samples with different wettability values yielded important information about the fluid distributions and surface properties. These two samples experienced different wetting features, although they were treated identically according to the flow chart in Fig. 3. In a previous investigation [12], the reason for this discrepancy may have been due to the geology and mineralogy of the samples. Sample B was acquired from the formation close to the source reservoir, grew chlorite films in the rocks, and contained more carbonate minerals trending toward oil-wetness. As a result, sample B exhibits a more oil-wet behavior behaves than sample A.

In the D-T_2 map, the blue horizontal line represents the water intrinsic diffusion line, which equal to the diffusion coefficient of the brine used with a salinity of 8000 ppm; the red inclined line represents the alkane diffusion line. In the T_1-T_2 map, the blue and red diagonal lines represent $T_1 = T_2$ and $T_1/T_2 = 1.6$, respectively. The D-T_2 maps of the used crude oil shown in the top right insets of Figs. 4(b and c) and 5(b and c), and T_1-T_2 maps shown in the bottom right insets of Figs. 4(e and f) and 5(e and f) are presented for reference.

Fig. 4 shows the NMR response of a core sample in the water-wet case. The oil and water peaks were separable in the D-T_2 domain. The intensity of the water signal changed with water saturation (S_w) as shown in Fig. 4(a–c). The water signal was located below the water line due to the restricted diffusion. With the decrease of water saturation from Fig. 4(a) to (c), the water signal gradually moved far away from

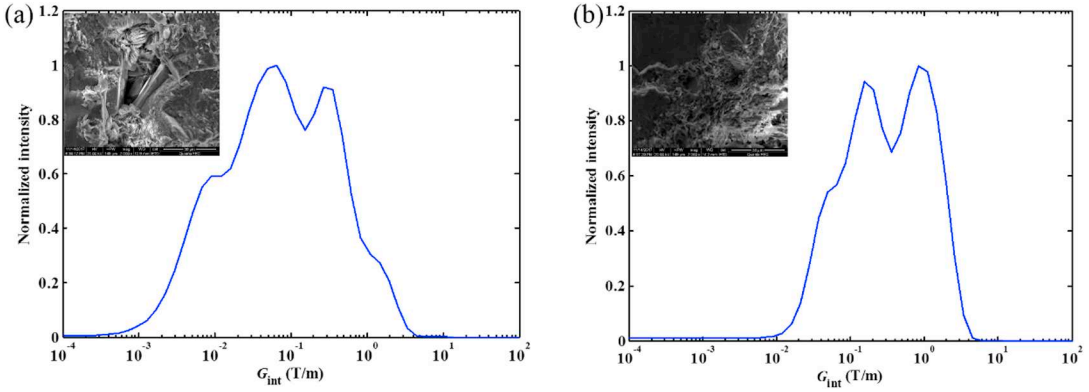

Fig. 2. The internal gradients distributions of (a) sample A ($\Delta\chi = 41.31 \times 10^{-6}$ SI) and (b) sample B ($\Delta\chi = 41.31 \times 10^{-6}$ SI). The top left insets show SEM micrographs of the sandstones.

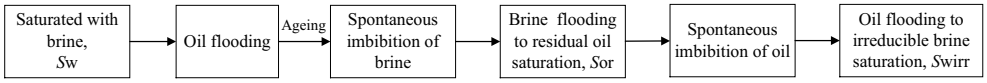

Fig. 3. Typical saturation cycle for the Amott test [22].

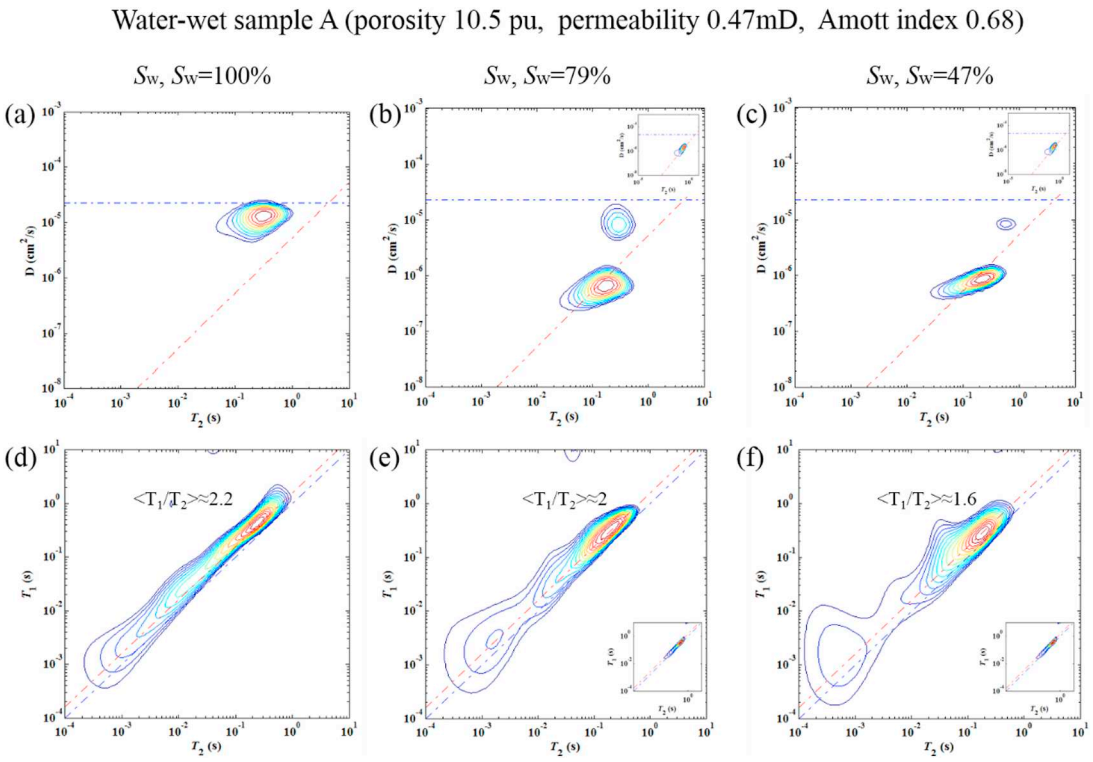

Fig. 4. Distributions of D-T_2 and T_1-T_2 of a water-wet sample at three saturation states. The top right insets show D-T_2 maps of the bulk crude oil. The bottom right insets show T_1-T_2 maps of the bulk crude oil. (For interpretation of the references to color in this figure, the reader is referred to the web version of this article.)

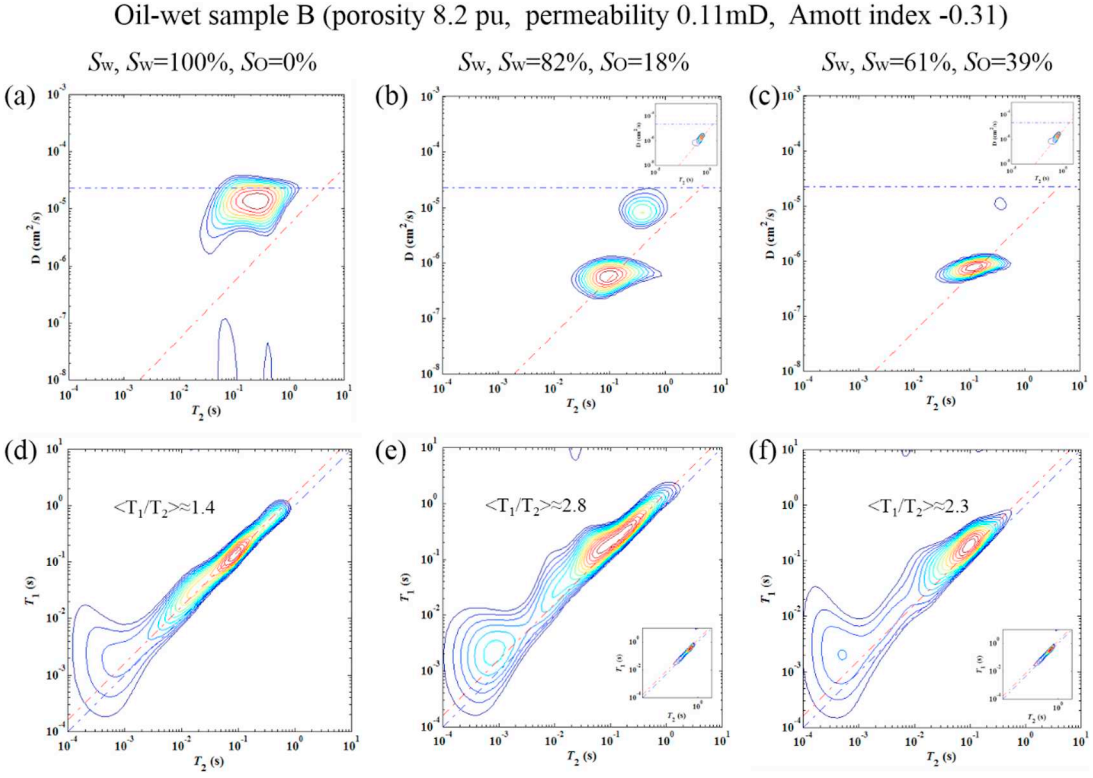

Fig. 5. Distributions of D-T_2 and T_1-T_2 of an oil-wet sample at three saturation states. The top right insets show D-T_2 maps of the bulk crude oil. The bottom right insets show T_1-T_2 maps of the bulk crude oil. (For interpretation of the references to color in this figure, the reader is referred to the web version of this article.)

the water line. The restricted diffusion phenomenon of the wetting water then became more obvious. In addition, the wetting water signal shifted to a short relaxation time on the T_2 axis; this happened because as the water saturation decreased, the ratio of the effective surface area and volume of pore space in the sample wetted by water gradually increased. However, the oil signal moved along the oil line in the direction of the decreasing diffusion coefficient in the D-T_2 map when compared to the bulk oil. Additionally, the changes in the diffusion axis were greater than those in the relaxation direction.

The corresponding T_1-T_2 datasets are presented in Fig. 4(d–f). The peak location was far away from T_1-T_2 parity, thus indicating that fluids were in contact at the pore surface [23]. In Fig. 4(d), the movable water signal located in the region of the T_1/T_2 ratio far exceeded 1.6. With the decrease of water saturation, the total signal of water and oil moved toward the region between the blue and red line in Fig. 4(e). At the S_{wirr} state, the oil peak showed an evident decrease in the T_1/T_2 ratio (Fig. 4(f)). This indicates that the independent water peak had a higher T_1/T_2 ratio than the oil signal on the basis of the relative changes. Therefore, this sample was deemed more water-wet based on theory and interpretations.

Comparison between the T_2 projection of the D-T_2 map and the T_2 distribution from the T_1-T_2 plot provides an estimate of the amount of the missing signal. This is a result of the signal attenuation during the PFG, and signals with a short T_2 cannot be detected. The missing signal relates to the micropores, (i.e., bound fluids). For this part of the signal, the T_1/T_2 ratio was almost higher than 1.6, which was indicative of probable water-wet conditions.

The D-T_2 and T_1-T_2 results for the oil-wet sample are presented in Fig. 5. The position of the water signal in the D-T_2 maps was always located away from the water line with changing water saturation. However, the observation that the oil signal gradually moved toward a short relaxation time in the T_2 projection of the D-T_2 map was not evident although the ratio of the effective surface area and volume of pore space occupied by wetting oil increased with the decrease of oil saturation (S_o) in Fig. 5(b and c). This could have been due to the relatively high oil saturation compared to movable water [24] or the oil viscosity. In addition, the diffusion coefficient of wetting oil in the sample decreased in comparison with bulk oil.

In the T_1-T_2 datasets for the oil-wet sample, for which water saturation amounted to 1, the water peak was located in the region between the blue line and red line. However, the main signal in Fig. 5(e and f) was far away from the red line despite the mixture of water and oil in S_{or} state. This indicated that oil with a high T_1/T_2 ratio in pores contributed to the wetting behavior.

Comparing D-T_2 and T_1-T_2 data in Fig. 4 with those in Fig. 5, whether water-wet or oil-wet conditions exist in tight rocks can be seen, the water signal showed an evident restriction diffusion phenomenon, yet the oil signal was observed wherein the decrease in the diffusion axis was greater than that in the relaxation direction with decreasing oil saturation. This could have been because the oil saturation was greater than the movable water saturation in pores. In addition, for the water-wet or oil-wet tight sand, the T_1/T_2 ratio of non-wet phase was rarely 1 for the bulk fluid. Therefore, interpretations will be made on the basis of relative changes in the water or oil T_1/T_2 ratios at different saturations.

4.2. NMR wettability results

Thus far, we have qualitatively discussed fluid distributions in the D-T_2 maps and the T_1/T_2 ratios in the T_1-T_2 plots for samples with different measured wettability index values. Then we conducted a quantitative wettability estimate using Eq. (3) and the D-T_2 maps acquired by the bipolar-STE-CPMG method. The surface relaxivities were determined by Eq. (4), as previously discussed. We obtained ρ_{effw} for the water results and ρ_{effo} of the oil data as an example (Fig. 6) at the saturation state of S_{or}. To increase the accuracy, m was measured using an electrical method. The standard wettability indices such as Amott

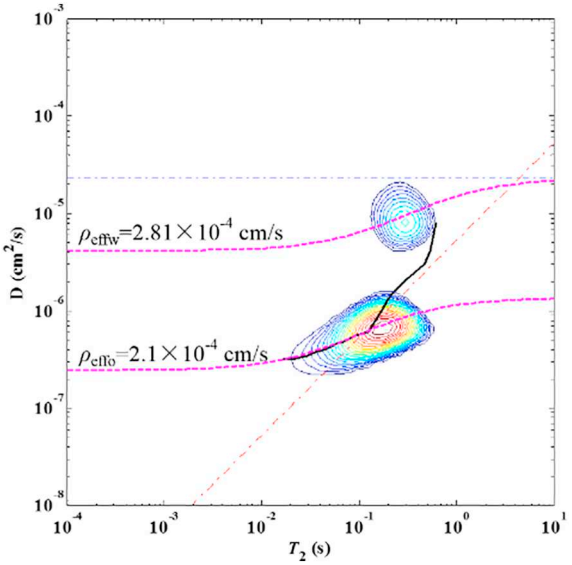

Fig. 6. Calculated ρ_{effw} and ρ_{effo} in the S_{or} state of sample A.

test results, were employed to test the calculated NMR wettability indicator. The ratio of ρ_{effw} and ρ_{effo} is given in two states. One represents the fully saturated case with the presence of one movable fluid. The other represents the partially saturated case (i.e., S_{or} state). The predicted NMR wettability results for the two cases were plotted along with the Amott wettability value in Fig. 7. Interestingly, the restored state results correlated better with the Amott tests than the results from the S_{or} state. This was likely related to the fact that the surface relaxivity estimation was influenced by water saturation. At the S_{or} state, relatively little water was present in the core sample, and therefore, the response of the rock to the water was ill-defined.

4.3. Wettability interpretation workflow

To address the challenge of wettability characterization using low-field NMR technique, we present a workflow for wettability interpretation using two-dimensional NMR data (Fig. 8). The wetting feature of the pores occupied with movable fluid in tight sand was validated using this workflow in the laboratory as discussed above. For the missing signal, i.e., the bound fluids with a T_2 less than 10 ms in the D-T_2 map, a T_1/T_2 ratio could be used to interpret the wettability. Effectively applying this approach remains an issue to be considered in a future study. It was noted that the Amott results matched to the NMR index results without the consideration of micropores. One possible reason for this is that the micropore fluids in a tight sample may have had difficulty spontaneously imbibing or displacing crude oil under the experimental conditions.

In downhole applications, obstacles may be encountered. The logging apparatus uses fixed field gradients (FFGs) rather than PFGs, but the proposed workflow should be effective for sandstones or carbonates without the effect of internal gradients. For tight sands, it may be necessary to build a correction model for internal gradients.

5. Conclusion

The relaxation behavior of tight sand samples is significantly affected by internal gradients, which are caused by various minerals and complex pore structures present in tight sand. The bipolar PFG-STE pulse sequence, which can eliminate the influence of the internal magnetic field gradient, was used to acquire D-T_2 maps to analyze the influence of wettability. Based on the obtained D-T_2 correlation maps, an applicable solution for wettability evaluation was provided. With the decrease of saturation, the wetting fluid signal moves toward a shorter

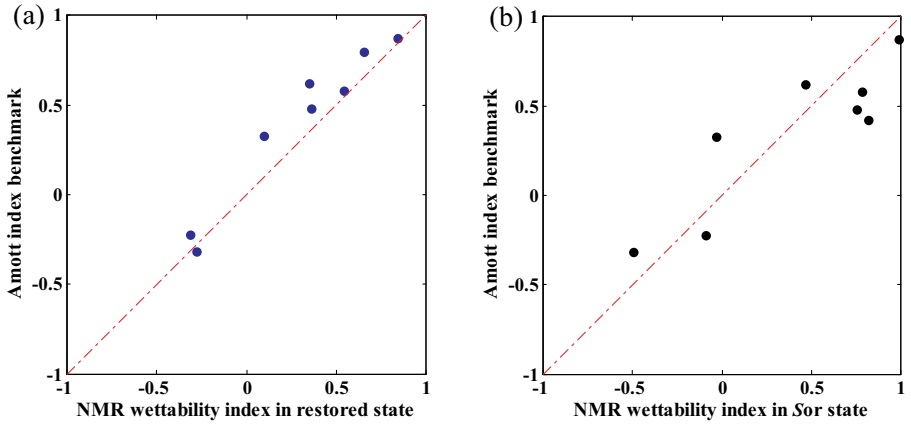

Fig. 7. The cross-plot of Amott test results and predicted wettability index values derived by using: (a) the ρ_{effw} and ρ_{effo} acquired from fully-saturated water and bound water states, respectively, and (b) the ρ_{effw} and ρ_{effo} calculated in the S_{or} case.

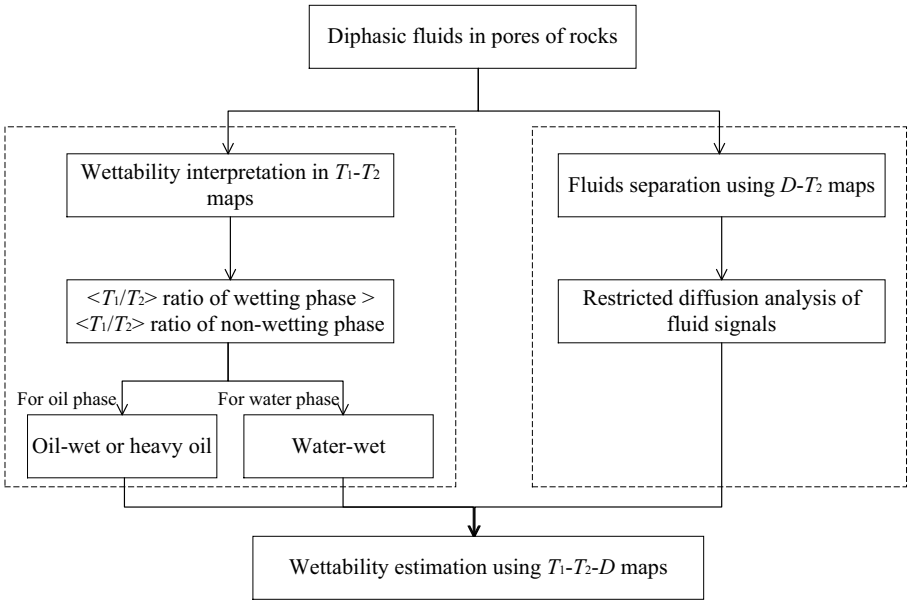

Fig. 8. The workflow for wettability interpretations of reservoir rocks.

relaxation time and a smaller diffusion coefficient in D-T_2 maps. Due to the effect of restricted diffusion, the wetting fluid can be accurately identified using the expanded restricted diffusion model. However, irrespective of if the wettability of the tight sandstone is in a water-wet or oil-wet state, the water phase always moves away from the free water diffusion line in tight sandstone D-T_2 maps.

The results of this study indicated that the obtained surface relaxivity using the restored case was better than that of the partial saturation case.

In addition, T_1-T_2 plots were presented as a complement for qualitative wettability analyses. It was shown that the T_1/T_2 ratio of the wetting phase increased relative to the value of the non-wetting phase in rocks. A workflow was also proposed to implement the wettability-determination technique based on two-dimensional NMR, and this workflow can be used even in downhole applications. The new method involves low cost and is more capable of assessing tight sand.

Acknowledgements

This work was supported by the National Natural Science Foundation of China (Grant No. 21427812) and the National “111 Project” (B13010).

References

[1] Hsu WF, Li X, Flumerfelt RW. Wettability of porous media by NMR relaxation methods. SPE Annual Tech Conf Exhib, Washington, DC. Oct 1992. p. 4–7.
[2] Young III T. An essay on the cohesion of fluids. Philos Trans R Soc Lond 1805;95:65–87.
[3] Song Y-Q. Magnetic resonance of porous media (MRPM): a perspective. J Magn Reson 2013;229:12–24.
[4] Howard JJ. Quantitative estimates of porous media wettability from proton NMR measurements. Magn Reson Imaging 1998;16:529–33.
[5] Zhang G-Q, Huang C-C, Hirasaki GJ. Interpretation of wettability in sandstones with NMR analysis. Petrophysics 2000;41:223–33.
[6] Freedman R, Heaton N, Flaum M, Hirasaki GJ, Flaum C, Hürlimann M. Wettability, saturation, and viscosity from NMR measurements. SPEJ 2003;8:317–27.
[7] Xiao L-Z, Liu H-B, Deng F, Zhang Z-F, An T-L, Zong F-R, et al. Probing internal gradients dependence in sandstones with multi-dimensional NMR. Microporous Mesoporous Mater 2013;178:90–3.
[8] Washburn KE, Eccles CD, Callaghan PT. The dependence on magnetic field strength of correlated internal gradient relaxation time distributions in heterogeneous materials. J Magn Reson 2008;194(1):33–40.
[9] Leu G, Fordham EJ, Hürlimann MD, Frulla P. Fixed and pulsed gradient diffusion methods in low-field core analysis. Magn Reson Imaging 2005;23(2):305–9.
[10] Chen J, Hirasaki GJ, Flaum M. NMR wettability indices: effect of OBM on wettability and NMR responses. J Pet Sci Eng 2006;52:161–71.
[11] Minh CC, Crary S, Singer PM, Valori A, Bachman N, Hursan G, et al. Determination of wettability from magnetic resonance relaxation and diffusion measurements on fresh-state cores. Society of Petrophysicists and Well-log Analysts 56th Annual

Logging Symposium, California, USA. Jul 2015. p. 18–22.
[12] Liang C, Xiao L-Z, Zhou C-C, Wang H, Hu F-L, Liao G-Z, et al. Nuclear magnetic resonance relaxation mechanisms and wettability characterization in low-permeability reservoirs. J Pet Sci Eng 2018. [submitted for publication].
[13] Cotts RM, Hoch MJR, Sun T, Markert JT. Pulsed field gradient stimulated echo methods for improved NMR diffusion measurements in heterogeneous systems. J Magn Reson 1989;83(2):252–66.
[14] Seland JG, Sørland GH, Zick K, Hafskjold B. Diffusion measurements at long observation times in the presence of spatially variable internal magnetic field gradients. J Magn Reson 2000;146(1):14–9.
[15] McDonald PJ, Korb J-P, Mitchell J, Monteilhet L. Surface relaxation and chemical exchange in hydrating cement pastes: a two-dimensional NMR relaxation study. Phys Rev E 2005;72:011409.
[16] Korb J-P, Freiman G, Nicot B, Ligneul P. Dynamical surface affinity of diphasic liquids as a probe of wettability of multimodal porous media. Phys Rev E 2009;80:061601.
[17] Valori A, Hursan G, Ma SM. Laboratory and downhole wettability from NMR T_1/T_2 ratio. Petrophysics 2017;58(04):352–65.
[18] Fleury M, Deflandre F. Quantitative evaluation of porous media wettability using NMR relaxometry. Magn Reson Imaging 2003;21:385–7.
[19] Zielinski L, Ramamoorthy R, Minh CC, Al Daghar KA, Sayed RH, Abdelaal AF. Restricted diffusion effects in saturation estimates from 2D diffusion-relaxation NMR maps. SPE Annual Tech Conf Exhib, Florence, Italy. Sep 2010. p. 19–22.
[20] Chen Q, Marble AE, Colpitts BG, Balcom BJ. The internal magnetic field distribution, and single exponential magnetic resonance free induction decay, in rocks. J Magn Reson 2005;175(2):300–8.
[21] Sun B, Dunn KJ. Probing the internal field gradients of porous media. Phys Rev E Stat Nonlinear Soft Matter Phys 2002;65(1):051309.
[22] Venkataramanan L, Hurlimann MD, Tarvin JA, Fellah K, Aeero-Allard D, Seleznev NV. Experimental study of the effects of wettability and fluid saturation on nuclear magnetic resonance and dielectric measurements in limestone. Petrophysics 2014;55:572–86.
[23] Mitchell J, Broche LM, Chandrasekera TC, Lurie DJ, Gladden LF. Exploring surface interactions in catalysts using low-field nuclear magnetic resonance. J Phys Chem C 2013;117:17699–706.
[24] Guo J-F, Xie R-H, Zou Y-L, Ding Y-J. Numerical simulation of multi-dimensional NMR response in tight sandstone. J Geophys Eng 2016;13(3):285.